RESEARCH PAPER

In Vitro Anti-cancer Potential of *Simarouba glauca* Phytochemical Constituents against Breast Cancer: Using Molecular Docking and Simulation Approach

Vanitha Subburaj[1], UmaaKuppuswamy*[2], Veintramuthu Sankar[3], Maida Engels SE[4], Vijayalakshmi Chinniah[5], Manju Velmurugan[6]

[1, 2, 3,4]PSG College of Pharmacy, Coimbatore-04, Tamil Nadu, India.
[5]Periyar College of Pharmaceutical Sciences, Tiruchirappalli
[6]Karpagam Faculty of Medical Sciences and Research, Coimbatore-04, Tamil Nadu, India.
Affiliated to the Tamil Nadu Dr. M G R Medical University.

Corresponding Author E-mail id: umaagangadhararao@gmail.com

Corresponding Author Address:
Dr. Umaa K
Professor & HOD
Department of Pharmaceutical Chemistry
PSG College of Pharmacy
Coimbatore-641004
E-mail: umaagangadhararao@gmail.com

Abstract

Breast cancer is the second most prevalent malignancy and the leading cause of cancer-related mortality among women worldwide, highlighting the need for novel therapeutic agents. Natural products, particularly plant-derived phytochemicals, are promising candidates for anticancer drug discovery. This study employed an integrated *in silico* and *in vitro* approach to evaluate the anticancer potential of *Simarouba glauca* phytoconstituents targeting estrogen receptor alpha (ERα-3ERT), progesterone receptor (PR-1SQN), and HER2/neu (3PP0). Molecular docking using the Glide module of Schrödinger Maestro assessed binding affinities and interactions, followed by molecular dynamics simulations for stability analysis. Drug-likeness and pharmacokinetic properties were predicted using QikProp.Docking results identified PR as the most favorable target, with glaucarbolone, amarolide, and ailanthone demonstrating strong binding affinities (−12.095, −10.868, and −10.868 kcal/mol, respectively) and the interaction throughpolar residues such as ASN719, LEU718, THR894 and GLN725 were observed. In contrast, moderate binding affinities were observed against ERα, with glaucarubinone through THR347 and LEU536 and dehydroglaucarubinone toward HER2/neu (−6.017 kcal/mol) via interactions with SER728, THR862, and ASP863. Molecular dynamics simulations confirmed the structural stability of the top-ranked glaucarbolone–PR complex, supporting its favorable binding mode. ADMET analysis revealed that all evaluated quassinoids complied with Lipinski's rule of five, and three exhibited favorable pharmacokinetic profiles.*In vitro* anti-proliferative studies demonstrated that *Simarouba glauca* leaf extract exhibits stronger activity against hormone-dependent breast cancer cells (MCF-7) compared to triple-negative cells (MDA-MB-231), with lower IC_{50} values (61.56 and 155.06 µg/mL, respectively). These findings highlight the potential of *Simarouba glauca* phytochemicals, particularly PR-targeting phytochemical compounds, as promising lead candidates for breast cancer therapy and underscore the effectiveness of integrated *in silico* approaches in early-stage anticancer drug discovery.

Keywords:
Breast Cancer Targets; ERα, PR, and HER2 / neu; SG phytochemicals; *In-silico* docking and ADMET property*;*

How to cite this article: Subburaj V, Kuppuswamy U, Sankar V, Engels SE M, Chinniah V, Velmurugan M. In Vitro Anti-cancer Potential of Simarouba glauca Phytochemical Constituents against Breast Cancer: Using Molecular Docking and Simulation Approach. Int J Drug Deliv Technol. 2026;16(76s): 40-54. DOI: 10.25258/ijddt.16.76s.5

Introduction

Breast cancer is a type of malignant growth that starts in the breast cells. The unchecked proliferation of cells within the breast tissue is the hallmark of this intricate and multidimensional disease [Łukasiewicz et al., 2021]. It is the second most prevalent cancer in women diagnosed globally and the second largest cause of cancer-related deaths in women [Sobhani et al., 2019]. Uncontrolled cell proliferation is the primary cause of breast cancer, which can be acquired or inherited during the course of a person's lifetime for a number of causes[Feng et al., 2018], including cellular changes like growth-inducing oncogenes beingactivated and tumour suppressor genes being inhibited, which interferes with cell proliferation and lead to unchecked cell growth[Hanahan& Weinberg., 2011]. Predisposing factors include female gender, hormone replacement treatment, late menopause, early menarche, lifestyle factors, exposure to chemicals and radiation, family history and prior diagnosis of breast cancer[Mayo Clinic., 2022].Genetic predispositions are hyperplasia, metaplasia and expression of hormone receptors such as ER (Estrogen Receptor) and HER2 (human epidermal growth factor receptor 2) [National Cancer Institute., 2021].

Breast cancer molecular subtypes are often divided into four subtypes based on the IHC profile. The first group is hormone receptor-positive breast cancer account for over 70% of cases [Orrantia-Borunda et al., 2022]: They are 1)luminal A (ER- and/or PR-positive, HER2-negative); 2)luminal B (ER- and/or PR-positive, HER2-positive or Ki67 > 14%); 3)HER2-enriched10–30% (HER2 amplified, ER- and PR-negative); and 4)Triple-negativebreast cancer (TNBC), which lacks the ER, PR, and HER2 receptors [Montagna et al., 2011]. Prognosis and survival are different according to these subtypes. Triple-negative and HER2-overexpressing tumors have been associated to the worst prognosis, while luminal tumors are associated with the best prognosis, but recurring breast cancer [Sorlie etal., 2001 & Carey et al., 2006]. Breast cancer mortality and incidence rates are rising daily due to the poor prognoses, ineffective treatment strategies and preventive measures to combat metastatic breast cancer [Łukasiewicz et al., 2021].

In modern treatments, patients are suffering more from medication resistance and cancer recurrence after receiving hormone treatment and traditional chemotherapy. Emergence of drug resistance and recurrence of cancer in conventional chemotherapy, hormone therapy, compromised immune system in radiation &surgery and also due to high cost and lead to increased cancer burden globally [Yue et al., 2019]. One such strategy to combat the global burden is to explore a good source of plant-derived novel anticancer phyto-molecules which are a compliment for chemotherapy and for the management and prevention of breast cancer [Jose et al., 2018]. Many researchers have directed their attention towards the development of novel anticancer molecules derived from natural sources due to their proven efficacy, tolerance, and mainly harmless nature towards normal cells, as well as their good sources and potential for use as powerful new antitumor agents in clinical practice [Hu et al., 2018].

Simarouba glauca (abbreviated as SG) is an evergreen anticancer medicinal plant that belongs to the Simaroubaceae family [Armour., 1959], also referred to as Laxmitaru or paradise tree and bitter damson princess tree are some of its common names. It is also known as "Tree of Solace of Cancer" since it is frequently utilized in the treatment of various cancers (Shyamsundar & Joshi., 2008).Since quassinoids, a class of triterpene phytochemical compounds that include canthinone as the alkaloid and ailanthinone, dehydro glaucarubinone, glaucarubine, glaucarubinone, holacanthone, melianone, simaroubidin, simarolide, simarubin, simarubolide, sitosterol, tirucalla, etc. are the main constituents of SG, they exhibit a wide range of inhibitory activities, including hepato-protective, anticancer, antiparasitic, antidysenteric, antipyretic, antimicrobial, antiprotozoal, antifungal, antioxidant, and antiulcer (Jose et al., 2020). Using target hunter databases and online server prediction, the current study evaluated the potential for breast cancer in *Simarouba glauca*.

Current study, the chosen SG phytochemicals (ligands) were permitted to interact with breast cancer targets like ERα, PR, and HER2 neu (PDBID: 3ERT, 1SQN, 3PP0) for their anticipated quassinoid inhibitory effects in order to investigate the biological activity. The current work looked into both traditional and novel ways for identifying new bioactive inhibitors from naturally occurring phyto-compounds. The *Simarouba glauca* plant's quassinoids are more likely to be employed as chemotherapeutic and preventive phytochemical compounds in the treatment of breast cancer. This study employed molecular docking, MD simulation, ADMET analysis and *in vitro* MTT assay for proving the anti breast cancer effect of SG.

2. Materials and Methods

2.1Softwares

The *in silico* studies were performed in the Schrödinger Maestro.

2.2 Ligand Selection and Preparation

After a comprehensive review of the literature, *Simarouba glauca's* phytochemical compounds were selected for this study. 3D structures of the selected SG phytochemicals (ligand) were obtained from the PubChem database, and they were prepared using the LigPrep module of Schrodinger [LigPrep, version 2.3, Schrodinger]. The SMILES of the selected ligands were imported into Maestro, version 9.0, Schrödinger. Transformation of 2D structures into low-energy three-dimensional (3D) structures was achieved by a module that generates possible stereoisomers, attaches hydrogens to the ligands, neutralizes charged structures and determines the most probable ionization state at the defined pH 7.0.

Due to the flexibility of most of the ligands, necessary steps were taken to consider a range of thermally accessible conformational states with the intention of increasing the chances of finding something close to the putative binding mode. The conformational space was explored by the combination of Monte-Carlo Multiple Minimum (MCMM)/ Low Mode (LMOD) with a maximum of 1000 conformers per structure and 100 minimization steps. Each minimized conformer was filtered by limiting 10 kJ mol^{-1} as a relative energy window, a value that sets energy threshold relative to the lowest-energy conformer and 1.00Å as a minimum atom deviation. Conformers with higher values than this threshold energy were discarded. All distances between pairs of corresponding heavy atoms were kept below 1.00 Å for two conformers to be considered identical.

2.3 Protein Preparation

The 3D crystal structures of ERα (PDB ID: 3ERT), PR (PDB ID: 1SQN), and HER2 receptor (PDB ID: 3PP0) were obtained from the Protein Data Bank (www.pdb.org/pdb) and subsequently employed in molecular docking studies to assess the interactions between phytochemicals from *S. glauca* and the chosen breast cancer targets (Halgren et al., 2004).The Protein Preparation Wizard of GLIDE (Grid-Based Ligand Docking with Energetic) was used to prepare them once they were imported into the Maestro workspace (Friesner et al., 2004). Glide uses a combination of rigid and flexible docking, maintaining the target protein's rigidity and the ligand molecules' flexibility. The protein preparation wizard offers many choices for adding potential missing hydrogen atoms to the PDB structure and assigning bond ordering. Ultimately, the OPLS3 force field and a 0.3 Å restrictions on the Root-Mean-Square Deviation (RMSD) of heavy atoms were used to complete the energetic optimization.

2.4 Grid Generation and Docking

After choosing the co-crystal ligand bound to the targets, the grid was generated using Glide's default settings. The inner grid box size was set to 10 Å, and the default center docking box can hold ligands with a length of ≤20 Å. The energy-minimized conformations were subjected to XP scoring, and the Glide scoring function (G-Score) was used for rescoring (Bowers et al., 2006).

2.5 Docking Validation

The docking process was confirmed by separating the ligand from each target and allowing Glide to re-dock into the active site with the default grid parameters. In order to guarantee that the inhibitor binds precisely to the active site cleft, it must exhibit little divergence from the real co-crystallized complex. The RMSD values between the co-crystallized ligand pose and the corresponding redocked pose were 3.5 Å, 3.2 Å, and 4.5 Å for the selected protein structures, respectively. These values fall within an acceptable range, indicating that the docking protocol reasonably reproduced the experimentally observed binding orientations.

2.6 Molecular Dynamics

Desmond Molecular Dynamics was used to perform the molecular dynamics simulations (Huang et al., 2011 & Yao et al., 2019). The Desmond System Builder application was employed to prepare the system after the ligand-target complex was first loaded. The TIP3P model produced explicit water molecules in an orthorhombic box used for the simulations (Harder et al., 2016). Steric conflicts are prevented by minimizing assemblies through the OPLS3e force field approach before the MD simulations. Desmond's Molecular Dynamics interface was then loaded with the finished configurations and simulations for 50 ns runs were started (Banks et al., 2005). The trajectory's recording interval was set at 1000 ps.

2.7 Drug Likeness Screening of SG Phytochemicals

The pharmacokinetic characteristics of bioavailability, BBB permeability, and toxicity were predicted and analyzed using the Qikprop (Lipinski et al., 2013) module of Maestro, Schrödinger (Jorgensen & Duffy., 2000). These include Polar Surface Area (PSA), CNS activity, Human Oral Absorption (HOA), and Lipinski's Rule of Five.

2.8 Evaluation of Anti-proliferative potentials of *Simarouba glauca* leaf extract

Anti-proliferative potential of *Simarouba glauca* aqueous leaf extract (SGALE) was assessed by *in vitro* MTT approach by inhibition of cell proliferation of human epidermal growth factor receptor 2 (HER2), progesterone receptor (PR), and estrogen receptor (ERα) statuses using MCF-7 and

MDA-MB-231cell lines after 24 h treatment separately [Puranik et al., 2017]. In this research, these cell lines were purchased from NCCS Pune, India, and were grown in Dulbecco's Modified Eagle Medium(DMEM) high-glucose medium. The culture was incubated in a CO_2 incubator at 37°C with a 5 % CO_2 atmosphere and 18–20 % O_2 for 24 h. 20,000 cells per well were seeded into 96-well plates.

The anti-proliferative effect was determined by introducing the reference (Doxorubicin-1µM/mL) and *Simarouba glauca* aqueous leaf extract (SGALE) at various concentrations (12.5, 25, 50, 100, and 200µg/mL). The plates were incubated for 24 h at 37ºC and then added 0.5 mg/mL MTT reagent to the entire volume. Cover the plate with aluminium foil to protect it from light and incubated for 3 h. Then, 100 µl DMSO was added to enhance solubility of MTT formazan crystals by gentle shaking in a gyratory shaker. A micro plate reader (Thermo Scientific, Multiskan GO Microplate Spectrophotometer) was used at 570 nm wavelength to detect absorbance. Percentage cell viability can be calculated using the formula below

$$\% \text{ Cell viability} = \frac{\text{Mean absorbance of treated cells}}{\text{Mean absorbance of untreated cells}} \times 100$$

The IC_{50} value was calculated using a linear regression equation.

$$Y = Mx + C$$

Where, Y =50, M and C values are taken from the viability

The percentage (%) of cell viability of treated groups such as SGALE at different concentrations (12.5, 25, 50, 100, and 200 µg/mL), as well as the positive (doxorubicin-1µM/mL) and negative controls (no drug treatment) on MCF7 and MDA MB-231 cells separately. Inhibitory concentration (IC_{50}) values were calculated for SGALE after 24 h incubation.

3. Result and Discussion

The popularity of medicinal plants is growing due to their unique qualities as an abundant resource of therapeutic phytochemicals that could be explored by the discovery of novel drugs [Nasimet al., 2022]. The success of naturally occurring anti-cancer medications recently, along with traditional medicine, has encouraged the scientific community to look for promising phytochemicals for treatment of various ailments [Yinet al., 2013]. *Simarouba glauca,* known as the "tree of solace of cancer", is a member of the Simaroubaceae family, and its leaf decoction was used in traditional medicine [Manasa et al., 2019] to treat both the first and second stages of cancer and increase the survival rate of patients with third and fourth stages of various cancers. Quassinoids are a class of bitter triterpene chemical compounds that have been shown to exhibit cytotoxic effects [Fiaschettiet al., 2011 &Vikas et al., 2017]. Recent discoveries addressing the numerous cancers with a single therapy have resulted in the emergence of drug resistance and treatment failure [Jose et al., 2018]. The current scenario experiences a surge in interest for the plant-based anticancer drugs for complementary treatment against breast cancer [Das &Agarwal., 2023].

A review of the literature on *Simarouba glauca* phytochemical compounds (quassinoids) revealed that more scientific molecular docking investigations may be useful for treating a variety of illnesses. Molecular docking and ADME analysis were examined for the anti-HIV1 potential of quassinoids from *Simarouba glauca* in previous docking research [Sameer &Sudhakar., 2020]. The compounds (2) cyanidin-3-O-(2-galloyl)-galactoside, (3) kaempferol-3-Oglucoside, and (4) kaempferol-3-O-pentoside displayed promising binding energies against yeast alpha glucosidase that were superior to acarbose (-6.867 kJ/mol) [Mugaranja & Kulal., 2020]. Anticancer properties of quassinoids showed from SG against PI3K inhibitors [Ramya et al 2018]. In contrast, gemcitabine (-188.48), cisplatin (-45.26), and thiotepa (-190.89) are common drugs. With a binding energy of (-248.25), canthin-6-one showed the highest binding affinity with a molecular target (EGFR-tyrosine kinase), as predicted [Prajapati&Reddy., 2017). Based on these results, canthin-6-one could be a suitable ligand for cancer treatment. Bioactive chemicals from *Simarouba glauca* leaf extracts were analyzed using molecular docking and ADMET to determine their anti-inflammatory and antioxidant properties (Aljawobaei et al., 2025).

3.1 Molecular Docking studies

3.1.1 SG Phytochemicals against Breast Cancer Targets

The physicochemical characteristics and 2D structures of chosen SG phytochemicals (ligands) that were retrieved from the PubChem database were shown in Figure.

Figure1: 2D structure of selected SG phytochemicals (ligands) with standard drugs

Docking Studies of *SG* Phytochemicals against Estrogen Receptor

Molecular docking was performed to evaluate the interaction of *SG* phyto constituents with three key breast cancer targets - ER-α (3ERT), PR (1SQN), and HER2 (3PP0)—which collectively regulate hormone responsiveness and tumor aggressiveness. Table 1 shows the docking scores

and binding affinities of *Simarouba glauca* (SG) phyto constituents toward the chosen estrogen receptor-α (ER-α; PDB ID: 3ERT), a validated therapeutic target in hormone-dependent breast cancer. 2D structures of SG Phytochemicals with Standard drugs are furnished in figure 1. Glaucarubinone surface view, 2D interactions, and 3D binding mode are shown in Figure 2 (a, b, and c). The ligand-receptor binding strength was estimated by applying the kcal/mol, where more affinity was indicated by more negative values. Currently prescribed drugs anastrozole (−8.853 kcal/mol) and gemcitabine (−8.144 kcal/mol) also showed strong interactions with the ER-α receptor, whereas tamoxifen displayed the highest binding affinity (−10.736 kcal/mol), indicating the robustness of the molecular docking analysis.

Among the SG phytoconstituents, melianone (−6.080 kcal/mol), glaucarubinone (−5.941 kcal/mol), glaucarubine (−5.638 kcal/mol), and ailanthinone (−5.316 kcal/mol) exhibited moderate yet favorable binding within the ER-α active site, suggesting their potential to interact with the estrogen receptor. Dehydroglaucarubinone showed weaker affinity (−4.357 kcal/mol), while fraxidin displayed minimal interaction (−0.716 kcal/mol), and several compounds did not exhibit significant docking under the applied conditions. Overall, these findings indicate that selected SG phytoconstituents possess appreciable ER-α binding potential, although lower than standard anti-estrogen drugs, supporting their consideration as promising lead scaffolds for further *in vitro*, *in vivo*, and mechanistic investigations in breast cancer therapy.

The ligand (glaucarubinone) exhibited a stabilized binding orientation within the binding pocket of ER-α (PDB ID: 3ERT) through key hydrogen bonds with residues such as THR347 and LEU536. Surface and shape analyses revealed deep pocket penetration with minimal solvent exposure and optimal intermolecular distances (1.86 – 2.50 Å), indicating efficient cavity occupancy. The interaction pattern resembles that of selective estrogen receptor modulators (SERMs), suggesting glaucarubinone may exhibit SERM-like modulation of ERα activity and serve as a promising natural scaffold for further validation.

S. no	Ligands	Pubchem ID	ERα (PDB ID: 3ERT)	PR (PDB ID: 1SQN)	Her 2 (PDB ID: 3PP0)
1	Ailanthone	72965	-	-10.868	-
2	Ailanthinone	44559321	-5.316	-5.565	-
3	Dehydroglaucarubinone	459112	-4.357	-s	-6.017
4	Glaucarubine	441794	-5.638	-	-6.509
5	Glaucarubinone	441796	-5.941	-	-4.761
6	Glaucarubolone	441797	-	-12.095	-
7	Amarolide	460539	-	-10.868	-
8	Simarolide	3081377	-	-	-
9	Holacanthone	158475	-	-6.920	-
10	Fraxidin	3083616	-0.716	-	-7.225
11	Melianone	99981	-6.08	-	-5.409
12	Gemcitabine	60750	-8.144	-8.744	-
13	Tamoxifen	2733526	-10.736	-	-5.108
14	Anastrazaole	2187	-8.853	-	-6.181

Table 1: Docking scores and binding affinities of *Simarouba glauca* phytochemicals with Breast cancer targets

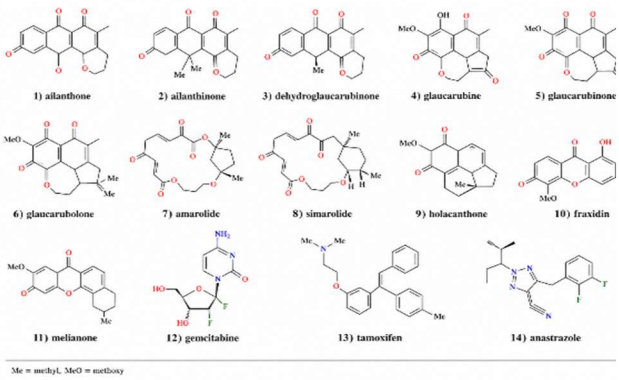

Figure 1: 2D structures of SG Phytochemicals with Standard drugs 1) ailanthone 2) ailanthinone, 3) dehydroglaucarubinone, 4) glaucarubine, 5) glaucarubinone, 6) glaucarubolone, 7) amarolide, 8) simarolide, 9) holacanthone, 10) fraxidin, 11) melianone, 12) gemcitabine, 13) tamoxifen, 14) anastrazaole

The binding affinity and docking scores of selected *Simaroubaglauca* (SG) phytochemicals with progesterone receptor (PR; PDB ID: 1SQN) were assessed, and results were shown in Table 1. The 3D binding mode, 2D interactions and surface view of glaucarbolone, amarolide, and ailanthone with the 1SQN target were illustrated in Figure 3 (a& b) Docking scores revealed that glaucarubolone exhibited the highest affinity for PR (−12.095 kcal/mol), exceeding that of the reference drug gemcitabine (−8.744 kcal/mol), while Ailanthone and Amarolide also showed strong binding (−10.868 kcal/mol each), indicating excellent compatibility with the PR ligand-binding domain. Holacanthone (−6.920 kcal/mol) and Ailanthinone (−5.565 kcal/mol) displayed moderate interactions, whereas other phytochemicals of SG did not show significant binding, suggesting receptor selectivity among the screened compounds.

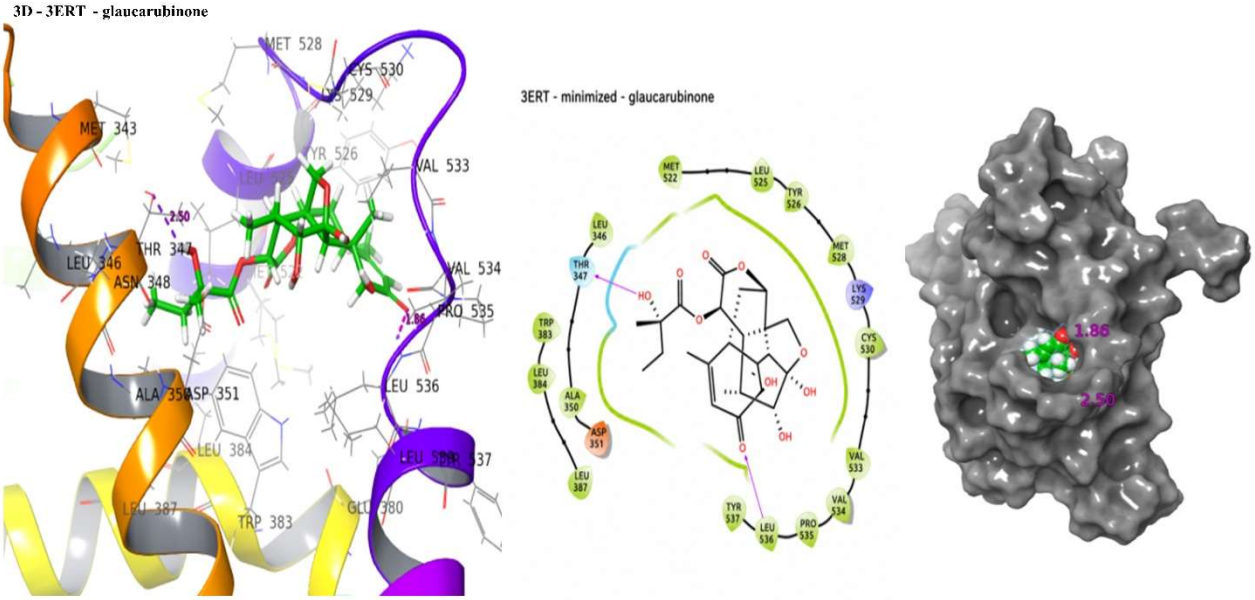

(a) **(b)** **(c)**

Figure 2 (a, b, & c): 3D, 2D interactions and Surface view of Glaucarubinone with 3ERT **(a)** 3D binding mode of glaucarubinone within the ligand-binding domain of ERα (PDB ID: 3ERT) (**b)** 2D interaction diagram illustrating hydrogen bonding and hydrophobic interactions between glaucarubinone and ERα residues. **(c)** Surface representation of ERα showing pocket occupancy and shape complementarity of glaucarubinone.

Docking Studies of *SG* Phytochemicals against Progesterone Receptor

Interaction analysis of 1SQN with glaucarbolone, amarolide, and ailanthone revealed that the selected SG quassinoid compounds exhibited stable binding conformations within the active site of the target protein, demonstrating favorable ligand–receptor interactions. The 3D interaction profiles showed that the ligands were well accommodated within the hydrophobic binding pocket, surrounded by key residues forming a stable environment. The 2D interaction diagrams further confirmed that the ligand was stabilized within the protein binding pocket through multiple interactions, predominantly hydrogen bonds with polar residues such as ASN719, LEU718. The binding site architecture shows a well-

defined pocket that accommodates the ligand through a combination of polar and non-polar interactions. Surface representation indicates that the ligand is deeply embedded within a partially polar cavity, with surrounding regions displaying complementary electrostatic potential that favorable stable protein–ligand binding. Overall, these results indicate that the studied compounds possess significant binding potential, which may contribute to their biological activity and supports their further consideration as promising candidates for drug development.

Figure 3 (a &b): 3D, 2D Interactions and Surface view of Glaucarbolone, Amarolide, Ailanthone with 1SQN (a): 3D binding modes of glaucarbolone, amarolide, and ailanthone within the active site of 1SQN. (b) 2D interaction maps highlighting hydrogen bonding and hydrophobic contacts between

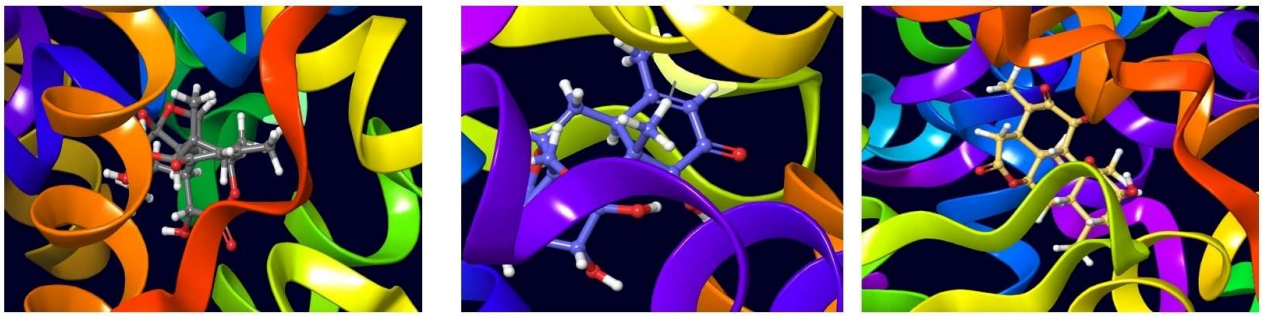

(a)

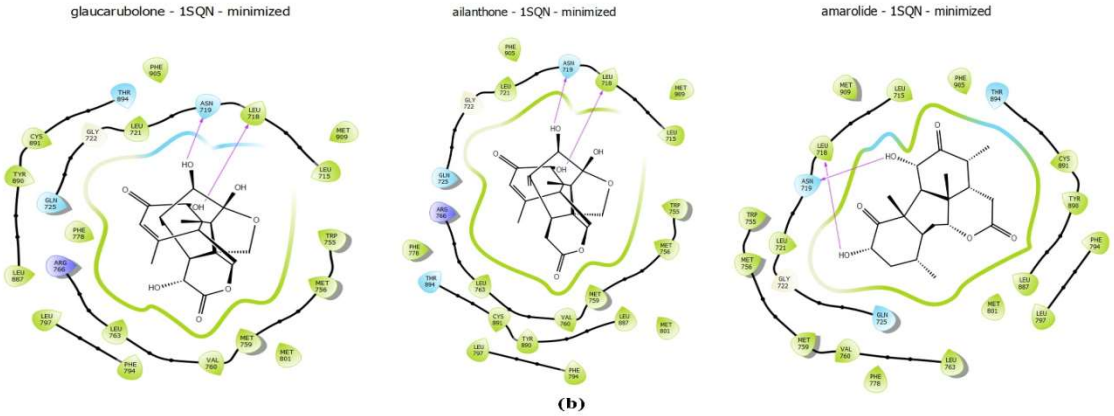

(b)

quassinoids and key 1SQN residues.

Docking Studies of *SG* Phytochemicals against HER2 receptor

The binding potential of selected SG phytoconstituents toward human epidermal growth factor receptor-2 (HER2; PDB ID: 3PPO), a significant oncogenic driver in aggressive and therapy-resistant breast cancers, was evaluated and docking scores indicated (Table 1) that fraxidin exhibited the strongest interaction with HER2 (−7.225 kcal/mol), followed by glaucarubine (−6.509 kcal/mol) and the reference drug anastrozole (−6.181 kcal/mol), suggesting moderate affinity within the HER2 binding region. Dehydroglaucarubinone (−6.017 kcal/mol) and melianone (−5.409 kcal/mol) also showed appreciable interactions, whereas glaucarubinone and tamoxifen displayed comparatively weaker binding.

Interaction results of dehydroglaucarubinone with 3PPOdemonstrated that the ligand was stabilized by hydrogen bonding with polar residues such as SER728, THR862, and ASP863. The surface view suggests that the ligand is embedded within a moderately polar binding pocket with complementary electrostatic features that support stable protein–ligand binding. Figure 4 (a, b, & c) showed the 3D binding mode, 2D interactions and surface view of dehydroglaucarubinone with 3PPO target. Overall, the combination of hydrogen bonding, hydrophobic, and electrostatic interactions indicates strong binding potential of the ligand, supporting its possible biological activity and highlighting its promise as a

potential lead compound for further drug development studies.

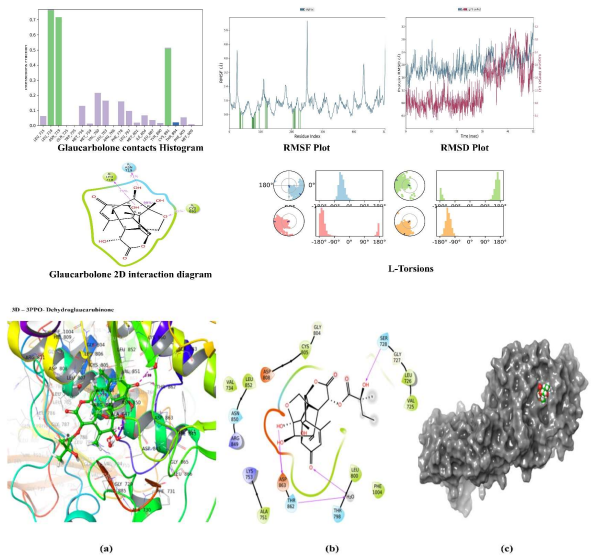

Figure 4 (a, b, & c): 3D, 2D interactions and Surface view of Dehydroglaucarubinone with 3PPO **(a)** 3D binding mode of dehydroglaucarubinone within the active site of 3PP0. **(b)** 2D interaction diagram showing hydrogen bonding and hydrophobic contacts between dehydroglaucarubinone and key residues of 3PP0. **(c)** Surface representation of 3PP0 highlighting pocket occupancy and shape complementarity of dehydroglaucarubinone.

Comparative docking analyses across ERα (3ERT), HER2 (3PP0), and PR (1SQN) demonstrated that quassinoids including glaucarubinone, dehydroglaucarubinone, glaucarbolone, amarolide, and ailanthone share a conserved binding paradigm dominated by their rigid polycyclic scaffold, which is deeply embedded within elongated hydrophobic cavities and stabilized primarily by extensive Vander Waals interactions. Target specificity is imparted through distinct hydrogen-bonding patterns, with ERα binding through key hydrogen bonds with residues such as THR347 and LEU536, HER2 binding stabilized by polar interactions involving SER728, THR862, and ASP863, and PR predominantly binding with polar residues such as ASN719, LEU718, through hydrogen bonds. Surface analysis shows high pocket occupancy and limited solvent exposure across all complexes, with variations in cavity filling between polar and hydrophobic quassinoids indicating tunable binding energetics. Overall, the quassinoid scaffold exhibited a conserved hydrophobic recognition mode complemented by target-specific polar interactions, supporting its potential for multi-target or optimized therapeutic development.

3.2 Molecular Dynamics Simulation Studies

The *in silico* validation was done by molecular dynamic studies using Desmond, Schrodinger to analyse the interactions established and stability of the target-ligand complex. Generally, RMSD and RMSF are used to evaluate the stability of the target-ligand complex. The RMSD of the Glaucarubinone-3ERT complex for a 50 ns timeline was found to be 3.5 Å, which is equal to the RMSD of the protein alone and shows that the interactions made by Glaucarubinone favors the stability (Figure 5). The Root-mean-square fluctuation (RMSF) is a plot of fluctuations of each residue versus the simulation timeframe, and the stability is inversely proportional to RMSF. The RMSF of Glaucarubinone-3ERT complex was found to be in the range of 0.8 to 4.8 Å. The simulation interaction diagram and ligand contact histogram obtained from MD studies were used to analyse the ligand target interaction from the perspective of ER α-Glaucarubinone agonist activity of Glaucarubinone. It illustrates water-mediated hydrogen bonding of Glaucarubinone with HIS 524which indicates the compactness of Glaucarubinone in the binding site.

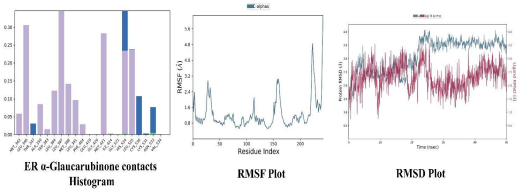

Figure 5: Molecular dynamic simulation parameters of Glaucarubinone-3ERT (ERα)

The RMSD of the Glaucarbolone -1SQN (**PR**) complex for a 50 ns timeline was found to be 3.2 Å, which is equal to the RMSD of the protein alone and shows that the interactions made by Glaucarbolone favors stability (Figure 6). The Root-mean-square fluctuation (RMSF) is a plot of fluctuations of each residue versus the simulation timeframe, and the stability is inversely proportional to RMSF. The RMSF of Glaucarbolone -1SQN (**PR**) complex was found to be in the range of 0.8 to 5.6 Å. The simulation interaction diagram and ligand contact histogram obtained from MD studies were used to analyse the ligand target interaction from the perspective of 1SQN (PR)-Glaucarbolone agonist activity of Glaucarbolone. It illustrates hydrogen bonding between Glaucarbolone and LEU 718, ASN 719, THR 894 and CYS 891of PR with 75%, 71% and 49% of the simulation time, respectively.

Figure 6: Molecular dynamic simulation parameters of Glaucarbolone-1SQN (PR) complex

The RMSD of the Dehydroglaucarubinone-3PP0 complexfor a 50 ns timeline was found to be 4.5 Å, which is equal to the RMSD of the protein alone and shows that the interactions made by Dehydroglaucarubinone favours the stability (Figure 7). The Root-mean-square fluctuation (RMSF) is a plot of fluctuations of each residue versus the simulation timeframe, and the stability is inversely proportional to RMSF. The RMSF of Dehydroglaucarubinone-3PP0 complexwas found to be in the range of 0.6 to 4.8 Å. The simulation interaction diagram and ligand contact histogram obtained from MD studies were used to analyze the ligand target interaction from the perspective of 3PP0-Dehydroglaucarubinoneagonist activity of Dehydroglaucarubinone. It illustrates water-mediated hydrogen bonding of Dehydroglaucarubinone with ASP 863 for 34% of the simulation time. In addition to this another hydrogen bonding was established between phenolic hydroxyl and ASP 863 for 84% of the simulation time which indicates the compactness of Dehydroglaucarubinone in the binding site.

Figure 7: Molecular dynamic simulation parameters of Dehydroglaucarubinone-3PP0 complex

3.3 ADMET Prediction

3.3.1 Drug Likeness and Lipinski Rule of Five

#stars is a score that shows how many of a molecule's calculated physicochemical and pharmacokinetic characteristics are outside the ideal range for 95% of known medications. A chemical is more likely to be "drug-like" and have a higher projected ADMET profile if it has a low #stars value (recommended 0–5), whereas a high number signals the molecule is less "drug-like." According to Schrodinger's ADMET prediction, all of the compounds demonstrated drug-likeness since the qikprop module's descriptors, such as lower #stars, lower MW, moderate logP, donor/acceptor H-bond counts, and rotatable bonds, were determined to be within the suggested range (Table 2).

Table 2: Drug likeness descriptors of SG phytochemicals

Ligands	**#stars (0-5)**	**mol MW (< 500 amu)**	**donorHB <5**	**acceptHB <15**	**log Po/w <5**	**#rotor <15**	**Rule of Five <2**
Glaucarubinone	0	494.5	4	12.65	0.842	7	**0**
Glaucarubin	0	496.5	5	12.35	1.052	8	**0**
Ailanthone	0	376.4	3	9.9	0.393	3	**0**
Ailanthinone	0	478.5	3	11.9	1.377	6	**0**
Amarolide	0	364.4	2	10.4	0.351	2	**0**
Simarolide	1	504.6	1	13.7	0.632	4	**1**
Dehydroglaucarubinone	0	492.5	4	12.65	0.715	7	**0**
Glaucarubolone	0	394.4	4	11.6	-0.261	4	**0**
Halocanthone	0	436.4	3	11.9	0.366	4	**0**
Fraxidin	0	222.1	1	4.75	1.054	3	**0**
Melianone	0	470.3	1	7.4	4.879	1	**0**

#stars, number of property descriptors outside the range observed for 95% of known drugs; mol MW, molecular weight; donor HB, hydrogen bond donors; accept HB, hydrogen bond acceptors; log P o/w, octanol/water partition coefficient; #rotor, number of rotatable bonds. Rule of Five indicates the number of violations of Lipinski's drug-likeness criteria.

3.3.2 Rule of Three

For any molecule to have oral absorption, intestinal membrane permeability is an essential parameter. The rule of three of the prenylated

phytoestrogens was predicted to analyse the Gut-blood barrier permeability. The compounds showed QPPCaco permeability in the order of Melianone > Fraxidin > Ailanthinone > Amarolide > Holacanthone > Glaucarubin > Glaucarubolone > Glaucarubinone > Simarolide > Dehydroglaucarubinone. When HOA and PHOA are observed, melianone, fraxidin and glaucarubin showed excellent oral absorption with 100%, 85% and 70%, respectively. As QPlogS is a measure of aqueous solubility of a compound, higher the value permeability is reduced. The results revealed that SG phytochemical compounds are considerably permeable and have good bioavailability and satisfy the rule of three and indicate their good permeability (Table 3).

Table 3: Rule of three parameters of *Simarouba glauca* phytochemicals

Ligands	QPP Caco	Oral Absorption		QP Log S	# metab	PSA	Rule of three
		HOA	PHOA				
Glaucarubinone	94.053	3	67.197	-3.205	6	167.472	0
Glaucarubin	119.445	2	70.283	-3.348	7	162.742	1
Ailanthone	149.45	3	68.168	-2.73	6	128.006	0
Ailanthinone	199.357	3	75.91	-3.455	6	148.657	0
Amarolide	135.042	3	67.134	-2.858	4	124.25	0
Simarolide	65.922				4		
Dehydroglaucarubinone	63.997	2	63.456	-3.058	7	176.491	1
Glaucarubolone	96.074	3	60.901	-2.397	5	144.079	0
Halocanthone	121.69	3	66.412	-2.839	5	154.148	0
Fraxidin	791.651	3	84.994	-1.894	3	77.21	0
Melianone	2149.001	3	100	-6.19	3	65.064	1

QPP Caco, predicted Caco-2 cell permeability; PSA, polar surface area; QP logS, predicted aqueous solubility;
#metab, predicted number of metabolic reactions

3.3.3 CNS Activity

To find out the ability of SG phytochemicals on CNS, QPlogBB and QPPMDCK were predicted and analyzed (Table 4). QPlogBB descriptor is used to predict the ability of BBB permeability, and the acceptable range is from -3.0 to 1.2. Low CNS penetration (CNS = −2), a profile that may be advantageous for non-CNS targets. QPPMDCK is used to predict the BBB permeability, and the poor BBB permeability is indicated by a QPPMDCK value of <25 and good BBB permeability is indicated by >50. As depicted in Table 4, the CNS activity, QPlogBB, QPPMDCK and PSA indicate the poor BBB permeability of SG phytochemicals. QPlog HERG, another toxicity descriptor in Schrödinger's QikProp, predicts a molecule's potential to block the hERG (human ether-à-go-go-related gene) potassium ion channel. However, most SG quassinoids showed acceptable hERG inhibition values (QPlogHERG> −5), indicating a low predicted risk of cardiotoxicity. All the phytochemical compounds showed low toxicity as the HERG inhibition is found to be below -5.6.

Table 4: CNS and toxicity descriptors of *Simarouba glauca* phytochemicals

Name of the SG Phytochemicals	**BBB permeability**			**Toxicity**		
	CNS	**QPlogBB**	**QPMDCK**	**QPLog HERG**	**#metab**	**#rtFG**
Glaucarubinone	-2	-1.684	38.432	-3.568	6	2
Glaucarubin	-2	-1.684	49.76	-3.693	7	2
Ailanthone	-2	-1.159	63.398	-3.224	6	2
Ailanthinone	-2	-1.361	86.564	-3.717	6	3
Amarolide	-2	-1.176	56.819	-3.147	4	2

Simarolide	-2	-1.638	26.173	-3.416	4	
Dehydroglaucarubinone	-2	-1.784	25.348	-3.465	7	2
Glaucarubolone	-2	-1.333	39.325	-2.887	6	2
Halocanthone	-2	-1.328	50.771	-3.255	5	3
Fraxidin	0	-0.556	384.306	-3.646	3	1
Melianone	0	-0.154	1130.989	-4.15	3	3

CNS, central nervous system activity; QP log BB, predicted brain/blood partition coefficient; QPMDCK, predicted Madin–Darby canine kidney cell permeability; QP log HERG, predicted HERG K^+ channel inhibition; #metab, predicted number of metabolic reactions; #rtFG, number of reactive functional groups; BBB, blood–brain barrier.

3.4 Evaluation of Anti-proliferative potentials of *Simarouba glauca* leaf extract

In vitro breast cancer results suggested that the SGALE was effective inhibition of cell viability in nature showed in Table 5, when compared to the standard (Doxorubicin) with IC_{50} values on the MCF7 cellline (61.56 µg/mL) and MDA MB-231cell showed 155.06 µg/mL, respectively, after the incubation of 24 h. The bar diagram (Figure 8) illustrated at different dose concentrations the inhibitory effect of SGALE treated with MCF7 and MDA MB 231 cells after 24 h and the direct microscopic observations were given in Figure 9 (a) & (b).

Anti-proliferative assay of SG aqueous leaf extract causes effective inhibition of cell viability in MCF7 with lower IC_{50} values than the MDA MB 231 cells in a dose-dependent manner, whereas moderate toxicity with a relatively low IC_{50} value was observed against the MDA MB 231 cells. Overall, the investigation found that SGALE had stronger anti-breast cancer properties and has proved to possess significantly low IC_{50} values against hormone-dependent breast cancer cells (MCF7) than the triple-negative breast cancer cell line (MDA MB-231) (61.56 and 155.06 µg/mL), respectively, which can be the best for utility as a phyto-molecule against breast cancer cells.

Table 5: Percentage Cell Viability of SG aqueous leaf extract against
MCF7 and MDA-MB 231 cells after 24 hours

Culture condition	**% Cell viability of *Simarouba glauca* aqueous leaf extracts (SGALE)**	
	MCF7 cells	**MDA-MB 231 cells**
Untreated	100±0.02	100±0.03
(Std) Dox-1 µM	46.13±0.03	44.92±0.02
12.5 µg	95.86±0.05	93.38±0.02
25 µg	77.58±0.09	86.35±0.01
50 µg	58.05±0.08	79.89±0.01
100 µg	32.83±0.02	67.74±0.02
200 µg	16.33±0.01	36.37±0.03
IC_{50} conc (µg/ml)	61.56 µg/ml	155.06 µg/ml

All the values are expressed ± SD (n=3)

Figure 8: Percentage cell viability of *Simarouba glauca* aqueous leaf extracts (SGALE) against MCF7 & MDA-MB cells after 24 hours

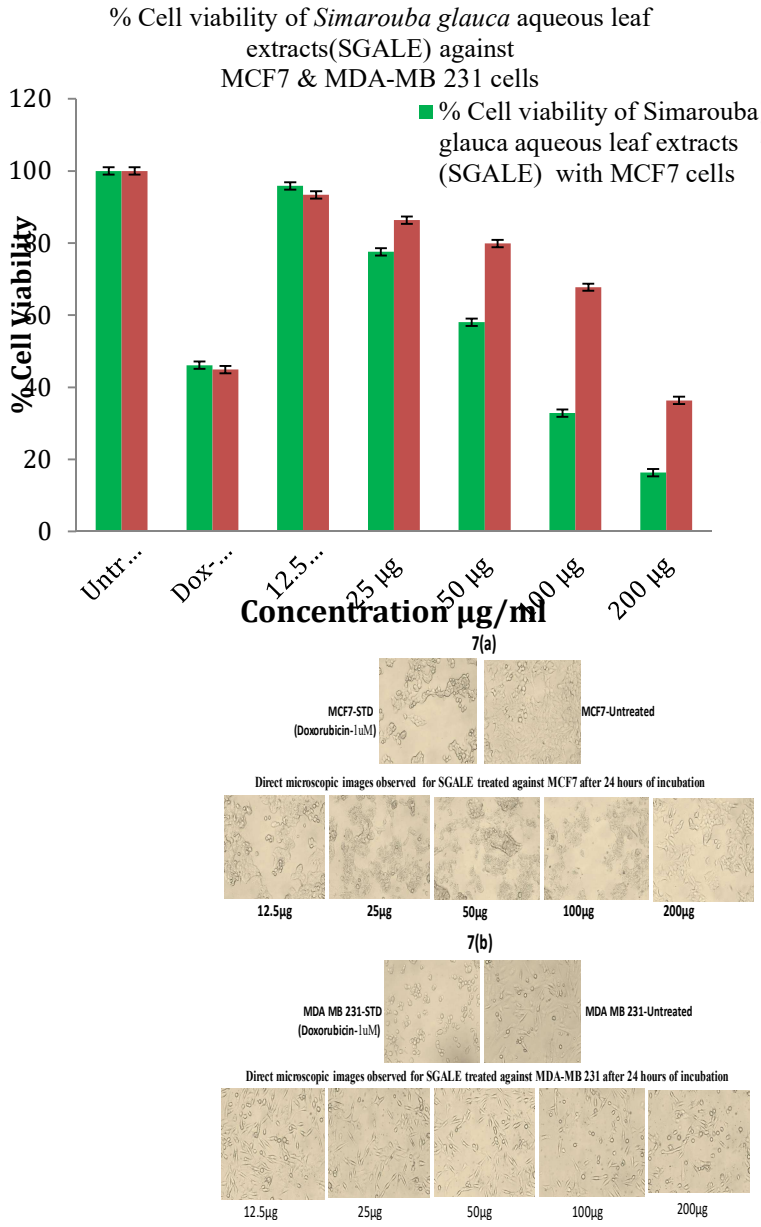

Figure 9 (a & b): Direct microscopic images observed for SGALE against
MCF7 and MDA-MB 231 after 24 hours

4. Conclusion

The present molecular docking, MD simulation and *in vitro* studied were demonstrated that *Simarouba glauca* phytochemical compounds had strong binding affinities and superior docking scores against key breast cancer targets (ER-α, PR, and HER2), with PR identified as the most favorable receptor. Quassinoids such as glaucarbolone, amarolide, and ailanthone exhibited notable affinity toward PR, suggesting their potential to modulate progesterone-dependent pathways and serve as promising lead molecules. ADMET analysis confirmed that all SG chemical compounds complied with Lipinski's Rule of Five, indicating favorable drug-likeness and pharmacokinetic profiles. Moderate activity against ER-α and limited but notable interactions with HER2 highlight possible multi-target potential of these phytoconstituents. Overall, the findings support the potential of *Simarouba glauca* phytochemicals as novel anticancer candidates, warranting further validation through detailed *in vitro* mechanistic and *in vivo* animal studies for therapeutic development.

5. Reference

1. Łukasiewicz S, Czeczelewski M, Forma A, Baj J, Sitarz R, Stanisławek A. Breast Cancer-Epidemiology, Risk Factors, Classification, Prognostic Markers, and Current Treatment Strategies-An Updated Review. Cancers (Basel). 2021;13(17):4287.
2. Sobhani N, D'Angelo A, Pittacolo M, Roviello G, Miccoli A, Corona SP, et al. Updates on the CDK4/6 inhibitory strategy and combinations in breast cancer. Cells. 2019;8(4):321.
3. Feng Y, Spezia M, Huang S, Yuan C, Zeng Z, et al. Breast cancer development and progression: Risk factors, cancer stem cells, signaling pathways, genomics, and molecular pathogenesis. Genes Dis. 2018;5(2):77-106.
4. Hanahan D, Weinberg RA. Hallmarks of cancer: the next generation. Cell. 2011;144(5):646-74.
5. Mayo Clinic. Breast cancer. 2022 [cited 2024 Jun 20]. Available from: https://www.mayoclinic.org/diseases-conditions/breast-cancer/symptoms-causes/syc-20352470
6. Loomans-Kropp HA, Umar A. Breast cancer prevention: Where are we now? Breast Cancer Res. 2019;21(1):47.
7. National Cancer Institute (NCI). BRCA Mutations: Cancer Risk and Genetic Testing. 2021 [cited 2024 Jun 20]. Available from: https://www.cancer.gov/about-cancer/causes-prevention/genetics/brca-fact-sheet
8. Orrantia-Borunda E, Anchondo-Nuñez P, Acuña-Aguilar LE, et al. Subtypes of Breast Cancer. In: Mayrovitz HN, editor. Breast Cancer. Brisbane (AU): Exon Publications; 2022. Chapter 3.
9. Montagna E, Bagnardi V, Rotmensz N, Viale G, Cancello G, Mazza M, et al. Immuno histochemically defined subtypes and outcome in occult breast carcinoma with axillary presentation. Breast Cancer Res Treat. 2011;129(3):867–75.
10. Sørlie T, Perou CM, Tibshirani R, Aas T, Geisler S, Johnsen H, et al. Gene expression

patterns of breast carcinomas distinguish tumor subclasses with clinical implications. Proc Natl Acad Sci U S A. 2001;98(19):10869–74.
11. Carey LA, Perou CM, Livasy CA, Dressler LG, Cowan D, Conway K, et al. Race, breast cancer subtypes, and survival in the Carolina Breast Cancer Study. JAMA. 2006;295(21):2492–502.
12. Yue GG, Wong LS, Leung HW, Gao S, Tsang JY, Lin ZX, et al. Evaluation of the safety profiles of estrogenic Chinese herbal medicines in breast cancer. Phytomedicine. 2019;56:103–17.
13. Jose A, Kannan E, Vijaya Kumar PR, Madhunapantula SV. Therapeutic Potential of Phytochemicals Isolated from *Simarouba glauca* DC for Inhibiting Cancers: A Review. Syst Rev Pharm. 2018;10(1):103-112.
14. Hu S, Xu Y, Meng L, Huang L, Sun H. Curcumin inhibits proliferation and promotes apoptosis of breast cancer cells. Exp Ther Med. 2018;16(2):1266–1272.
15. Armour RP. Investigations on kernels of *Simarouba glauca* Dc. in El Salvador. Econ Bot. 1959;13(1):41–66.
16. Shyamsundar J, Joshi S. *Simarouba glauca* DC (Paradise Tree). Department of Agricultural Economics, University of Agricultural Sciences, Bangalore: Conference Papers; 2008.
17. Jose A, Kannan E, Madhunapantula SV. Anti-proliferative potential of phytochemical fractions isolated from *Simarouba glauca* DC leaf. Heliyon. 2020;6(4):e03836.
18. Schrödinger Release 2021-3: LigPrep. New York, NY: Schrödinger, LLC; 2021.
19. Schrödinger Release 2011: QikProp, version 3.4. New York, NY: LLC; 2011.
20. Halgren TA, Murphy RB, Friesner RA, Beard HS, Frye LL, Pollard WT, et al. Glide: a new approach for rapid, accurate docking and scoring. 2. Enrichment factors in database screening. J Med Chem. 2004;47(7):1750–1759.
21. Friesner RA, Banks JL, Murphy RB, Halgren TA, Klicic JJ, Mainz DT, et al. Glide: a new approach for rapid, accurate docking and scoring. 1.Method and assessment of docking accuracy. J Med Chem. 2004;47(7):1739–1749.
22. Friesner RA, Murphy RB, Repasky MP, Frye LL, Greenwood JR, Halgren TA, et al. Extra precision glide: docking and scoring incorporating a model of hydrophobic enclosure for protein-ligand complexes. J Med Chem. 2006;49(21):6177–6196.
23. Bowers KJ, Chow DE, Xu H, Dror RO, Eastwood MP, Gregersen BA, et al. Scalable algorithms for molecular dynamics simulations on commodity clusters. In: Proceedings of the ACM/IEEE SC 2006 Conference (SC'06). Tampa, FL: IEEE; 2006.
24. Huang C, Li C, Choi P, Nandakumar K, Kostiuk LW. A novel method for molecular dynamics simulation in the isothermal isobaric ensemble. Mol Phys. 2011;109(2):191–202.
25. Yao C, Kang Z, Yu B, Chen Q, Liu Y, Wang Q. All-factor analysis and correlations on the transmembrane process for arginine-rich cell-penetrating peptides. Langmuir. 2019;35(28):9286–9296.
26. Harder E, Damm W, Maple J, Wu C, Reboul M, Xiang JY, et al. OPLS3: A force field providing broad coverage of drug-like small molecules and proteins. J Chem Theory Comp. 2016;12(1):281–296.
27. Banks JL, Beard HS, Cao Y, Cho AE, Damm W, Farid R, et al. Integrated modeling program, applied chemical theory (IMPACT). J Comp Chem. 2005;26(16):1752–1780.
28. Iványczi M, Balogh B, Kis L, Mándity I. Molecular dynamics simulations of drug-conjugated cell-penetrating peptides. Pharmaceuticals (Basel). 2023;16(9):1251.
29. Ivanova N, Ivanova A. Testing the limits of model membrane simulations-bilayer composition and pressure scaling. J Comput Chem. 2018;39(8):387–396.
30. Lipinski CA, Lombardo F, Dominy BW, Feeney PJ. Experimental and computational approaches to estimate solubility and permeability in drug discovery and development settings. Adv Drug Deliv Rev. 2012;64:4-17.
31. Jorgensen WL, Duffy EM. Prediction of drug solubility from Monte Carlo simulations. Bioorg Med Chem Lett. 2000;10(11):1155-1158.
32. Puranik SI, Ghagane SC, Nerli RB, Jalalpure SS, Hiremath MB. Evaluation of in vitro antioxidant and anticancer activity of *Simarouba glauca* leaf extracts on T-24 bladder cancer cell line. Pharmacogn J. 2017;9(6):906–912.
33. Nasim N, Sandeep IS, Mohanty S. Plant-derived natural products for drug discovery:

current approaches and prospects. Nucleus (Calcutta). 2022;65(3):399-411.
34. Yin SY, Wei WC, Jian FY, Yang NS. Therapeutic applications of herbal medicines for cancer patients. Evid Based Complement Alternat Med. 2013;2013:302426.
35. Manasa M, Palanimuthu DV, Suresha DKB, Munishamanna MK. Proximate and phytochemical analysis of an Anticancerous *Simarouba glauca* leaves. J Pharmacogn Phytochem. 2019;8(3):4224–4227.
36. Fiaschetti G, Grotzer MA, Shalaby T, Castelletti D, Arcaro A. Quassinoids: From traditional drugs to new cancer therapeutics. Curr Med Chem. 2011;18(3):316–328.
37. Vikas B, Akhil BS, Suja SR, Sujathan K. An Exploration of Phytochemicals from Simaroubaceae. Asian Pac J Cancer Prev. 2017;18(7):1765-1767.
38. Das A, Agarwal SM. Recent advances in the area of plant-based anti-cancer drug discovery using computational approaches. Mol Divers. 2023;28(2):901–25.
39. Sameer S, Sudhakar M. Molecular docking and ADME analysis for Anti - HIV1 potential of quassinoids from *Simarouba glauca*. J Pharmacol Clin Res. 2020;8(4):555742.
40. Mugaranja KP, Kulal A. Alpha glucosidase inhibition activity of phenolic fraction from *Simarouba glauca*: An in-vitro, in-silico and kinetic study. Heliyon. 2020;6(7):e04392.
41. Ramya KS, Iqbal S, Gunasekaran K, Radha A. Anticancer Potentials of Quassinoids from *Simarouba glauca* – Docking and ADME Analysis. Res J Life Sci Bioinform Pharm Chem Sci. 2018;4(5):2-15.
42. Prajapati C, Reddy MN. Molecular Docking Studies of Canthin-6-One from *Simarouba glauca* against EGFR Tyrosine Kinase. Int J Pharm Sci Res. 2017;8(12):5130-5136.
43. Aljawobaei W, Ali SSM, Thippeswamy NB, et al. Molecular docking and ADMET analysis of bioactive compounds from *Simarouba glauca* leaf extracts for anti-inflammatory and antioxidant activities. Discov Appl Sci. 2025;7:1082.
44. Razak NA, Abu N, Ho WY, Zamberi NR, Tan SW, Alitheen NB, et al. Cytotoxicity of eupatorin in MCF-7 and MDA-MB-231 human breast cancer cells via cell cycle arrest, anti-angiogenesis and induction of apoptosis. Sci Rep. 2019;9(1):1514.
45. Martyna A, Rosslein M, Claridge JK, et al. Conceptual framework for the optimization of isothermal-isobaric boundary parameters in nanoscale fluid bilayers. J Phys Chem B. 2011;115(4):803-812.
46. Sun L, Liang X, Gao J, Wang L. Mechanical transport mechanisms and lipid headgroup interactions of arginine-rich peptides: a multiscale simulation perspective. Biophys J. 2019;117(3):542-553.
47. Roos K, Wu C, Damm W, et al. OPLS3e: Extending Force Field Coverage for Drug-Like Small Molecules. J Chem Theory Comput. 2019;15(3):1863-1874.
48. Xie J, Wang Y, Zhang L. Molecular dynamic trajectories of therapeutic peptide-drug bioconjugates traversing complex biological membranes. J Control Release. 2023;361:214-225.

Acknowledgement: The authors are thankful to the Principal and Management, PSG and Sons' Charities for providing all the facilities and other research assistance towards the completion of this research work. The authors are thankful to Averin Biotech Labs-Bangalore for helping me to complete their research work. The authors are also thankful to The Tamil Nadu Dr MGR Medical University for the support given during the PhD research process.

Conflict of Interest: The authors declare that there is no conflict of interest

Abbreviations

ADMET-Absorption, Distribution, Metabolism, Excretion and Toxicity, ERα- estrogen receptor alpha, PR- progesterone receptor, HER2-Human Epidermal Growth Factor Receptor 2, GLN725-Glutamine 725, Thr862-Threonine 862, Asp863-Aspartic Acid 863, Ser728-Serine 728, Leu536-Leucine 536, MCF-Michigan Cancer Foundation, MDA-MB-231-**M**D **A**nderson-**M**etastatic **B**reast-231**,** IC_{50}- Half Maximal Inhibitory Concentration, SG- *Simarouba glauca*, National Cancer Institute-NCI, TNBC-Triple-negative breast cancer, MD-Molecular dynamics, MTT-3-(4,5-dimethylthiazol-2-yl)-2,5-diphenyltetrazolium bromide**,** 3D-Three-Dimensional**,** 2D-Two-Dimensional**,** (MCMM-Monte-Carlo Multiple Minimum, LMOD-Low Mode, kJ- kilojoule Å-Ångström, GLIDE-Grid-Based Ligand Docking with Energetic, PDB ID-Protein Data Bank Identifier, RMSD-Root-Mean-Square Deviation, XP-eXPerience, TIP3P-Transferable Intermolecular Potential with 3 Points, OPLS3e-Optimized Potentials for Liquid Simulations, 3rd Generation Extended, OPLS-AA-Optimized Potentials for Liquid Simulations-All Atom, NVT-Network Virtual Terminal, NPT-National Pipe Thread, PSA-Polar Surface Area, CNS-Central Nervous System, HOA-Human Oral Absorption,

NCCS-National Centre for Cell Science, DMEM-Dulbecco's Modified Eagle Medium, SGALE - *Simarouba glauca* aqueous leaf extract, DMSO-Dimethyl sulfoxide**,** EGFR- Epidermal Growth Factor Receptor, kcal/mol-kilocalories per mole, TYR526-Tyrosine526, LEU346-Leucine346, ALA350-Alanine350, VAL533-Valine533, PRO535-Proline535, PHE778-Phenylalanine, MET759-Methionine, TRP755-Tryptophan, ARG-Arginine, ASP-Aspartic acid, SERM-Selective Estrogen Receptor Modulator, RMSF-Root Mean Square Fluctuation, MW-Molecular Weight**,** QPPCaco-QikProp Predicted Apparent Caco-2 Cell, PHOA-Percent Human Oral Absorption, QPlogS-Predicted Aqueous Solubility, QPlogBB-Predicted Brain/Blood Partition Coefficient, QPPMDCK- Predicted Apparent Madin-Darby Canine Kidney (MDCK) Cell Permeability, BBB- Blood-Brain Barrier, rtvFG-Number of Reactive Functional Groups, QPlog HERG-human ether-a-go-go-related gene (hERG) potassium channels.